New Journal of Physics
The open-access journal for physics

Angular momentum decomposition of entangled photons with an arbitrary pump

Alison M Yao
SUPA and Department of Physics, University of Strathclyde, Glasgow G4 0NG, UK
E-mail: alison@phys.strath.ac.uk

New Journal of Physics **13** (2011) 053048 (12pp)
Received 23 December 2010
Published 24 May 2011
Online at http://www.njp.org/
doi:10.1088/1367-2630/13/5/053048

Abstract. We calculate the biphoton state generated by spontaneous parametric down-conversion in a thin crystal and under collinear phase matching conditions using a pump consisting of any superposition of Laguerre–Gauss modes. The result has no restrictions on the angular or radial momenta or, in particular, on the width of the pump, signal and idler modes. We demonstrate the strong effect of the ratio of the pump width to the signal/idler widths on the composition of the down-converted entangled fields. The knowledge of this ratio is shown to be essential for calculating the maximally entangled states that can be produced using pumps with a complex spatial profile.

Contents

1. Introduction

Quantum entanglement is one of the defining properties of quantum mechanics. It forms the basis of quantum information [1, 2] and quantum computing [3] and is essential for applications such as entangled cryptographic systems [4] and quantum imaging [5–8]. A great deal of the research in this area has focused on qubit quantum entanglement, although entanglement has also been demonstrated between spatial modes carrying orbital angular momentum (OAM) [9–11]. Since these modes are defined within an infinite-dimensional, discrete Hilbert space, there is considerable interest in their potential to generate multi-dimensional entangled states not only for the enhancement of the efficiency of current quantum protocols, but also for the realization of new, higher-dimensional quantum channels.

Spontaneous parametric down-conversion (SPDC), that is, the generation of two lower-frequency photons when a pump field interacts with a nonlinear crystal, has been shown to be a reliable source of photons that are entangled [12], in particular, in their OAM [9]. The spatial structure of the down-converted biphotons can be expressed as a superposition of Laguerre–Gauss (LG) modes of different amplitudes, angular and radial momenta, with the width of the modal expansion relating to the amount of entanglement of the final state. Both angular (ℓ) and radial (p) momenta can be controlled and converted between one another using diffractive optical elements, typically in the form of spatial light modulators (SLMs) displaying holograms [13–15]. Experimentally, detection of the down-converted modes is often done using single-mode fibres (SMFs), which accept only $\ell = p = 0$ modes [11], and SLMs are used to convert $|\ell| > 0$ modes to $\ell = 0$ modes. Note that SLMs affect both ℓ and p [13] and this should be taken into consideration.

In this paper, we calculate the exact analytical form of the biphotons for any LG pump, with no restrictions on the angular or radial momenta, ℓ and p, respectively, or, in particular, on the widths, w, of the pump, signal and idler modes. Our calculation demonstrates that OAM is conserved. We use our result to calculate the coincidence amplitudes of the LG modes in the generated two-photon entangled state for a variety of pump beams. We demonstrate the importance of the various beam sizes (the pump width and the choice of LG base for the signal and idler) in determining the state of the down-converted photon and the resulting ℓ distribution, also known as the quantum spiral bandwidth (SB) [16]. We find excellent agreement with previous analyses that considered more restricted conditions [16, 17].

The size of the emission modes $w_{s,i}$, and hence the choice of measurement basis, is dependent on the experimental setup being used. In particular, in many experiments (e.g. [11, 14, 15]), the widths are determined by the back-projected size on the crystal of the SMF used for detection. Although the fibres will project onto structures that approach a Gaussian, they are imaged onto the crystal via the SLM used in the detection process. Thus the image on the crystal will be an LG mode determined by the ℓ of the SLM. We allow the sizes of the emission modes to be free parameters in order to emphasize that these are experiment dependent. In this way, our result provides a recipe for calculating the down-converted state for any experimental configuration and, indeed, for finding the setup that would be required for producing a given down-converted state.

Knowledge of the exact form of the down-converted photons opens up the possibility of engineering the entangled modes, through an appropriate choice of the pump beam, in order to produce biphotons that are, for example, maximally entangled in some subspace [18]. We show how our result can be easily extended to pump beams that are complex superpositions

of LG modes, including pump modes containing phase singularities (PSs). We again see excellent agreement with previous analysis [18]. Moreover, by allowing the beam widths to be free parameters, we show that the pump to signal/idler size ratio plays a critical role in the engineering of the down-converted state, with states only being maximally entangled at particular width ratios.

2. Spontaneous parametric down conversion (SPDC) and spiral bandwidth (SB)

We consider a thin nonlinear crystal (typically 1–3 mm), tuned for type-I, collinear down-conversion, illuminated by a continuous-wave LG pump beam propagating in the z-direction and confined within the crystal and assume perfect phase matching. This produces two highly correlated, lower-frequency photons, commonly termed the signal and the idler. Since energy is conserved, $\omega_\mathrm{p} = \omega_\mathrm{s} + \omega_\mathrm{i}$, where the subscripts p, s and i refer to the pump, signal and idler, respectively.

The down-converted biphoton state in this case is given by [18, 19]

$$|\psi_\mathrm{SPDC}\rangle = \int \mathrm{d}r_\perp \Phi(r_\perp)\hat{a}_\mathrm{s}^\dagger(r_\perp)\hat{a}_\mathrm{i}^\dagger(r_\perp)|0,0\rangle, \tag{1}$$

where $\Phi(r_\perp)$ is the spatial distribution of the pump beam at the input face of the crystal, $|0,0\rangle$ is the vacuum state and $\hat{a}_\mathrm{s}^\dagger(r_\perp)$ and $\hat{a}_\mathrm{i}^\dagger(r_\perp)$ are creation operators for the signal and idler modes, respectively. The integral is over the plane perpendicular to the axis of the pump beam.

Since the photon pairs generated by SPDC are entangled in arbitrary superpositions of an infinite number of modes with OAM, they are best described by mode functions that are LG modes, LG_p^ℓ. At the beam waist ($z = 0$) the normalized LG modes are given, in cylindrical coordinates, by [20]

$$\mathrm{LG}_p^\ell(\rho,\phi) = \sqrt{\frac{2p!}{\pi\,(p+|\ell|)!}}\frac{1}{w}\left(\frac{\rho\sqrt{2}}{w}\right)^{|\ell|}\exp\left(\frac{-\rho^2}{w^2}\right)L_p^{|\ell|}\left(\frac{2\rho^2}{w^2}\right)\exp(\mathrm{i}\ell\phi). \tag{2}$$

Here w is the beam waist, ℓ corresponds to the angular momentum, $\ell\hbar$, carried by the beam and describes the helical structure of the wave front around a wave front singularity and $p+1$ describes the number of radial intensity maxima.

We can then write the biphoton state as

$$|\psi_\mathrm{SPDC}\rangle = \sum_{\ell_\mathrm{s},p_\mathrm{s}}\sum_{\ell_\mathrm{i},p_\mathrm{i}} C_{p_\mathrm{s},p_\mathrm{i}}^{\ell_\mathrm{s},\ell_\mathrm{i}}\,|\ell_\mathrm{s},\,p_\mathrm{s};\,\ell_\mathrm{i},\,p_\mathrm{i}\rangle\,, \tag{3}$$

where $P_{p_\mathrm{s},p_\mathrm{i}}^{\ell_\mathrm{s},\ell_\mathrm{i}} = |C_{p_\mathrm{s},p_\mathrm{i}}^{\ell_\mathrm{s},\ell_\mathrm{i}}|^2$ is the probability of finding one photon in the signal mode $|\ell_\mathrm{s},\,p_\mathrm{s}\rangle$ and the other in the idler mode $|\ell_\mathrm{i},\,p_\mathrm{i}\rangle$ given a pump mode $|\ell_\mathrm{p},\,p_\mathrm{p}\rangle$.

The coincidence amplitudes $C_{p_\mathrm{s},p_\mathrm{i}}^{\ell_\mathrm{s},\ell_\mathrm{i}}$ are calculated from the overlap integral

$$C_{p_\mathrm{s},p_\mathrm{i}}^{\ell_\mathrm{s},\ell_\mathrm{i}} = \langle\psi_\mathrm{i},\,\psi_\mathrm{s}|\psi_\mathrm{SPDC}\rangle \tag{4}$$

$$= \int_0^{2\pi}\mathrm{d}\phi\int_0^\infty \rho\,\mathrm{d}\rho\mathrm{LG}_{p_\mathrm{p}}^{\ell_\mathrm{p}}(\rho,\phi)\left[\mathrm{LG}_{p_\mathrm{s}}^{l_\mathrm{s}}(\rho,\phi)\right]^*\left[\mathrm{LG}_{p_\mathrm{i}}^{l_\mathrm{i}}(\rho,\phi)\right]^*. \tag{5}$$

Note that after substituting (2) into (5), the integral over the azimuthal coordinate is

$$\int_0^{2\pi} \mathrm{d}\phi \exp\left[\mathrm{i}\left(\ell_\mathrm{p} - \ell_\mathrm{s} - \ell_\mathrm{i}\right)\phi\right] = 2\pi\,\delta_{\ell_\mathrm{p},\ell_\mathrm{s}+\ell_\mathrm{i}}, \tag{6}$$

from which we obtain the well-known conservation law for OAM: $\ell_\mathrm{p} = \ell_\mathrm{s} + \ell_\mathrm{i}$ [9, 21].

Substituting this into (5) and using the associated Laguerre polynomial in the form [22]

$$L_\mathrm{p}^{|\ell|}(x) = \sum_{i=0}^{p} (-1)^i \frac{(p+|\ell|)!}{(p-i)!(|\ell|+i)!\,i!}\,x^i\,, \tag{7}$$

we obtain

$$\begin{aligned} C^{\ell_\mathrm{s},\ell_\mathrm{i}}_{p_\mathrm{s},p_\mathrm{i}} = \delta_{\ell_\mathrm{p},\ell_\mathrm{s}+\ell_\mathrm{i}} \sqrt{\frac{2}{\pi w_\mathrm{p}^2}} \frac{2^{\sigma_\ell+1}\gamma_\mathrm{s}^{|\ell_\mathrm{s}|+1}\gamma_\mathrm{i}^{|\ell_i|+1}}{\left(1+\gamma_\mathrm{s}^2+\gamma_\mathrm{i}^2\right)^{\sigma_\ell+1}} \sqrt{p_\mathrm{p}!p_\mathrm{s}!p_\mathrm{i}!\left(|\ell_\mathrm{p}|+p_\mathrm{p}\right)!\left(|\ell_\mathrm{s}|+p_\mathrm{s}\right)!\left(|\ell_\mathrm{i}|+p_\mathrm{i}\right)!} \\ \times \sum_{k=0}^{p_\mathrm{p}} \sum_{i=0}^{p_\mathrm{s}} \sum_{j=0}^{p_\mathrm{i}} \frac{(-2)^{k+i+j}\gamma_\mathrm{s}^{2i}\gamma_\mathrm{i}^{2j}}{\left(1+\gamma_\mathrm{s}^2+\gamma_\mathrm{i}^2\right)^{k+i+j}} \\ \times \frac{[\sigma_\ell+k+i+j]!}{(p_\mathrm{p}-k)!(|\ell_\mathrm{p}|+k)!k!(p_\mathrm{s}-i)!(|\ell_\mathrm{s}|+i)!i!(p_\mathrm{i}-j)!(|\ell_\mathrm{i}|+j)!j!}, \end{aligned} \tag{8}$$

where $\sigma_\ell = (|\ell_\mathrm{p}| + |\ell_\mathrm{s}| + |\ell_\mathrm{i}|)/2$ and $\gamma_\mathrm{s} = w_\mathrm{p}/w_\mathrm{s}$, $\gamma_\mathrm{i} = w_\mathrm{p}/w_\mathrm{i}$ are the ratios of the pump width to the signal/idler widths.

Equation (8) allows us to calculate the exact analytical form of the down-converted photons produced using any LG pump (or superposition thereof) with no restrictions on any of the beam parameters. The calculation of the coincidence amplitudes can also be used to calculate the number of OAM modes participating in the down-converted state, also known as the spiral bandwidth (SB).

3. Coincidence amplitudes and SB for special cases

For a given pump, equation (8) shows that the coincidence amplitudes have a strong dependence on the ratio of the pump width to the chosen widths of the LG bases for the signal and idler, γ_s and γ_i. Experimentally, the maximum width of the pump is limited by the size of the down-conversion crystal, while the widths of the signal and idler beams are determined by the size of the SMF used in the detection process. We can see this dependence more clearly if we consider some simplified examples.

3.1. A Gaussian pump, $\ell_\mathrm{p} = p_\mathrm{p} = 0$.

We first consider the simplest possible case: a Gaussian pump with $\ell_\mathrm{p} = p_\mathrm{p} = 0$ and biphotons with no radial dependence, i.e. $p_\mathrm{s} = p_\mathrm{i} = 0$. Moreover, we assume that the signal and idler modes have the same width s.t. $\gamma_\mathrm{s} = \gamma_\mathrm{i} = \gamma$. From the conservation of OAM, equation (6), we know that $\ell_\mathrm{s} = -\ell_\mathrm{i} = \ell$ in this case and so we can reduce equation (8) to

$$C^{\ell,-\ell}_{0,0} = \sqrt{\frac{2}{\pi w_\mathrm{p}^2}} \left(\frac{2\gamma^2}{1+2\gamma^2}\right)^{|\ell|+1}. \tag{9}$$

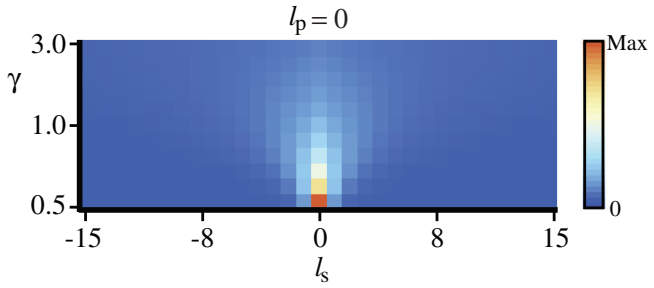

Figure 1. SB for a Gaussian pump with $\ell_p = p_p = 0$ and the fixed width $w_p = 1.0$ as a function γ.

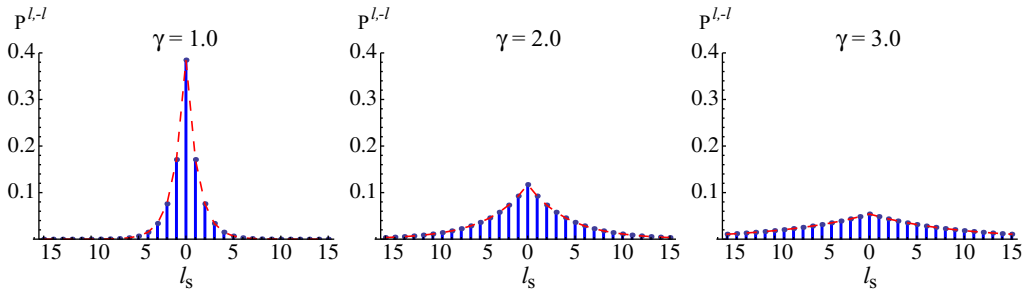

Figure 2. SB for a Gaussian pump with $\ell_p = p_p = 0$ and $w_p = 1.0$. The signal and idler widths are equal and reduced s.t. $\gamma = 1.0, 2.0, 3.0$ from left to right. Vertical (blue) lines were calculated using (9) and dashed (red) lines were calculated using equations (10) and (11) of [16].

It is clear that the SB depends only on the ratio of the pump width to the signal/idler widths, γ. As in previous works, for example [16, 17], this further reduces to

$$C_{0,0}^{\ell,-\ell} \propto \left(\frac{2}{3}\right)^{|\ell|} \tag{10}$$

when all the beam widths are the same, i.e. $\gamma = 1$.

The effect of γ on the SB is shown in figure 1, where we have plotted the SB as a function of γ. It can be seen that as the signal/idler widths are reduced w.r.t. the pump width (i.e. as γ increases), the SB increases but the amplitudes of the participating modes decrease. In figure 2 we plot (in blue) the SBs for $\gamma = 1.0$, 2.0 and 3.0. These results are in excellent agreement with previous works, see, for example, figure 1 of [16] (shown in red in figure 2). Note that throughout this work although we only plot the SB from $-15 \leqslant \ell \leqslant 15$, which are experimentally realizable values, we calculate the coincidence amplitudes for a much larger range of ℓ and use these results to 'normalize' the coincidence probabilities. The effect of different beam parameters on a Gaussian pump has been explored in detail recently [23]. In particular, the work [23] explores the effects of the radial nodes and shows that the coincidence probabilities are determined by the overlap of the signal and idler with the pump. The work [23] also shows that there is excellent agreement between the analysis for collinear systems, as presented here, and the analysis for non-collinear geometries in the approximation of a thin crystal.

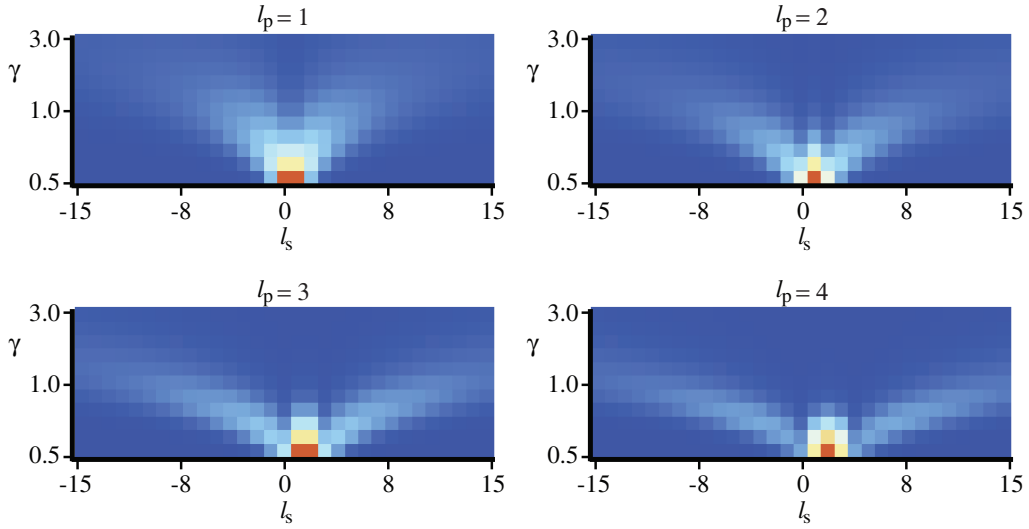

Figure 3. SB for LG pumps of fixed width $w_p = 1.0$ and $\ell_p = 1, 2, 3, 4$ as the signal/idler width is reduced s.t. $\gamma_s = \gamma_i$ goes from 0.5 to 3.0.

3.2. A Laguerre–Gaussian pump, $\ell_p > 0$.

We now consider what happens when the pump is a higher-order LG mode, i.e. $\ell_p > 0$. In this case the conservation of OAM requires $\ell_i = \ell_p - \ell_s$. As before, we start with the simplest case, $p_{p,s,i} = 0$. The probability amplitudes are then described by

$$C_{0,0}^{\ell_s,\ell_i} = \delta_{\ell_p,\ell_s+\ell_i}\sqrt{\frac{2}{\pi w_p^2}}\frac{2^{\sigma_\ell+1}\sigma_\ell!}{\sqrt{|\ell_p|!|\ell_s|!|\ell_i|!}}\frac{\gamma_s^{|\ell_s|+1}\gamma_i^{|\ell_i|+1}}{\left(1+\gamma_s^2+\gamma_i^2\right)^{\sigma_\ell+1}},$$

where $\sigma_\ell = (|\ell_p| + |\ell_s| + |\ell_i|)/2$. This agrees with equation (8) of [17] when using normalized LG modes and assuming that all the modes have the same width.

To see how the OAM of the pump affects the SB, we first calculate the coincidence probabilities, $P_{0,0}^{\ell_s,\ell_p-\ell_s}$, as a function of ℓ_s and γ for different values of ℓ_p. As figure 3 shows, the SB is symmetric around half the OAM value of the pump. For small values of γ the SB has a single maximum around $\ell_p/2$. As γ increases, however, the SB splits into two 'wings' for $\ell_p > 0$. These are still symmetric around $\ell_p/2$ and have maxima that depend on ℓ_p and γ. The physical explanation of this is that pump modes with $\ell_p > 0$ form rings whose diameters increase with both the value of ℓ_p and the width of the beam. Maximum overlap between the pump and the signal/idler modes, and hence maximum coincidence amplitudes, occurs therefore at larger values of ℓ_s and ℓ_i.

Next we consider what happens when the widths of the signal and idler are different. We find that by varying the ratio of the signal width to the idler width (in this case from $\gamma_i = 0.5\gamma_s$ to $2.0\gamma_s$) it is possible to fully suppress the SB for either negative or positive values of ℓ_s, as shown in figure 4.

Until now, we have considered only modes with no radial modes, i.e. $p_p = p_s = p_i = 0$. Higher-order LG beams are commonly produced using an SLM. Since these produce OAM modes with a range of radial indices, p [13], we now look at the effect that p has on the form of the spatial mode function of the entangled photons. We find that the number of 'wings'

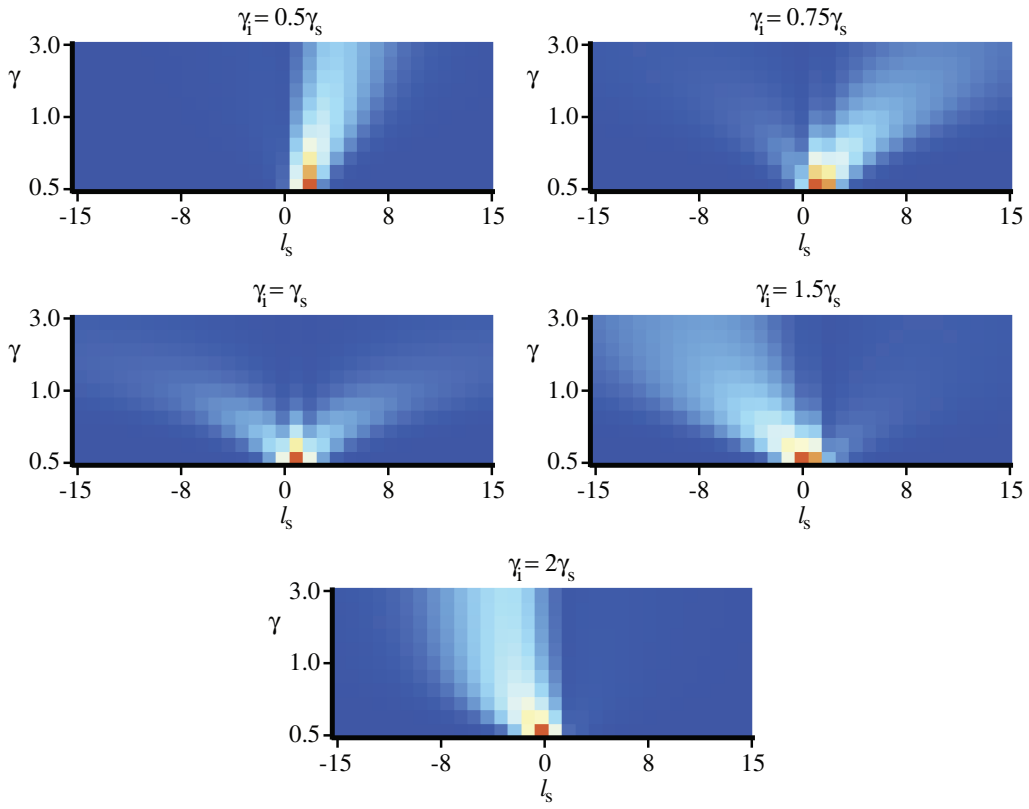

Figure 4. SB for a LG pump with $\ell_p = 2$ and $w_p = 1.0$ as the signal/idler width is reduced s.t. γ_s goes from 0.5 to 3.0. The signal and idler modes have different width ratios: $\gamma_i/\gamma_s = 0.5$, 0.75, 1.0, 1.5 and 2.0.

increases with the radial index of the pump as shown in figure 5. As before, altering the ratio of the signal width to the idler width suppresses one set of wings. Again these correspond to areas of maximum overlap between the pump and the signal/idler modes.

If we allow first our signal/idler beams to have non-zero radial modes and then all beams to have non-zero radial modes, the SB as a function of γ becomes ever more complex. The effect of the radial number of the pump is shown in figure 6.

3.3. Engineered entangled states

Entangling systems in higher-dimensional states is important for many quantum communication applications. Not only does the higher dimensionality imply a greater potential for applications in quantum information processing, but also it has been suggested that increasing the dimensionality of the entangled states of a system can make its non-classical correlations more robust to the presence of noise and other detrimental effects [24, 25]. Torres *et al* [18] have demonstrated (theoretically) that arbitrary engineered entangled states in any d-dimensional Hilbert space can be prepared using SPDC to translate the topological information contained in a pump beam into the amplitudes of the generated entangled quantum states. Controlling OAM state superpositions in this way engenders the ability to produce and manipulate quantum states with an arbitrarily large number of dimensions. Indeed, Torres *et al* illustrated this

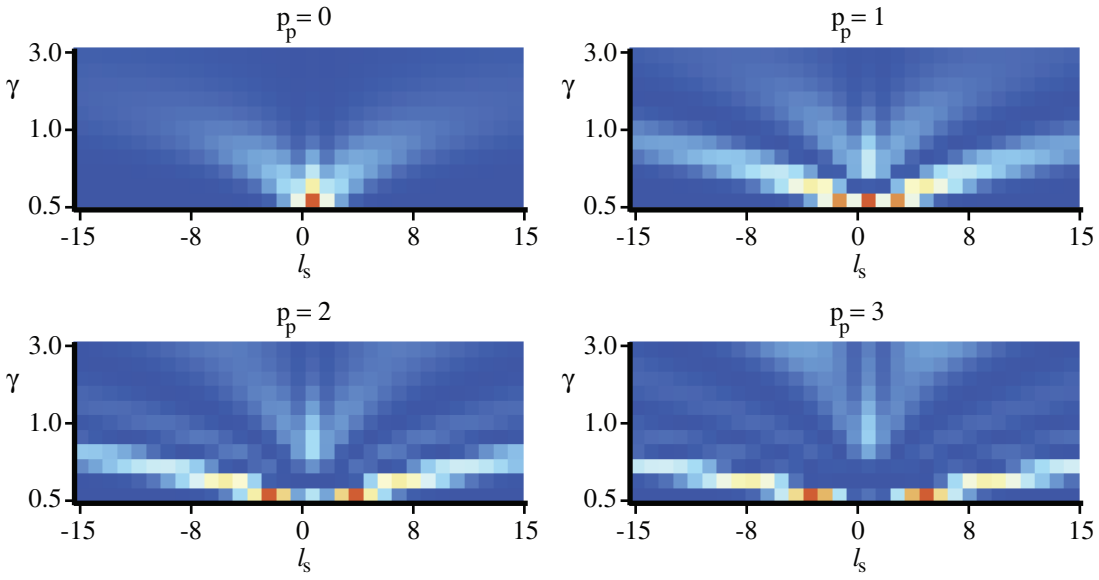

Figure 5. SB for a LG pump with $\ell_{\rm p} = 2$ and $w_{\rm p} = 1.0$ as the signal/idler width is reduced s.t. $\gamma_{\rm s} = \gamma_{\rm i}$ goes from 0.5 to 3.0. The radial number of the pump is increased from $p_{\rm p} = 0$ to 3.

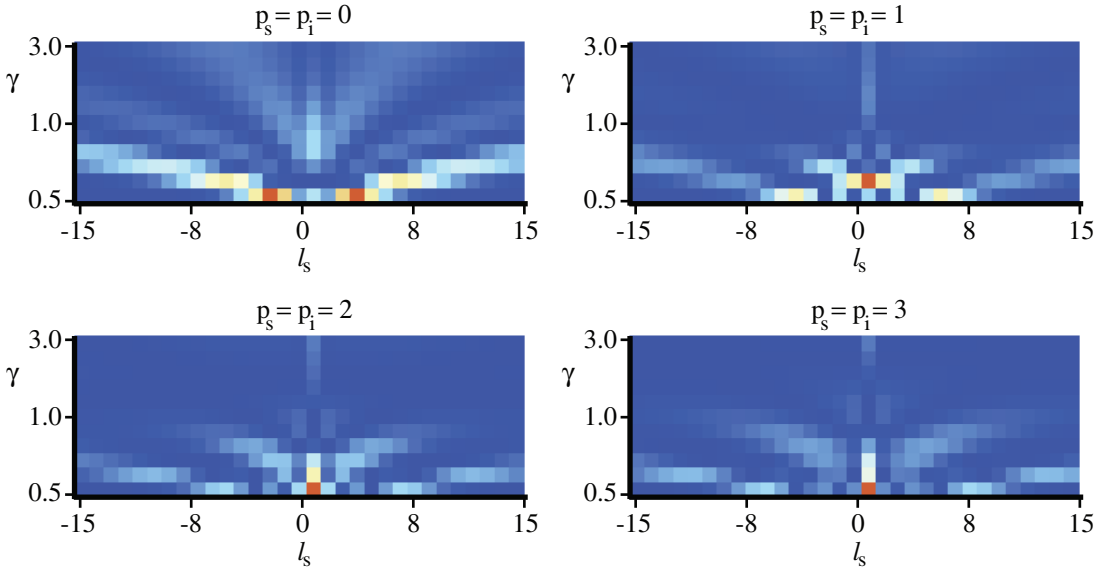

Figure 6. SB for a LG pump with $\ell_{\rm p} = p_{\rm p} = 2$ and $w_{\rm p} = 1.0$ as the signal/idler width is reduced s.t. $\gamma_{\rm s} = \gamma_{\rm i}$ goes from 0.5 to 3.0. The radial number of the signal and idler modes is increased from $p_{\rm s} = p_{\rm i} = 0$ to 3.

by calculating a number of maximally entangled states of different dimensions, produced using pump beams containing PSs. Here we describe how our results can be easily extended to such pumps, which can be described by complex superpositions of LG modes [26]. Moreover, we demonstrate that the ratio of the pump width to the signal/idler widths must

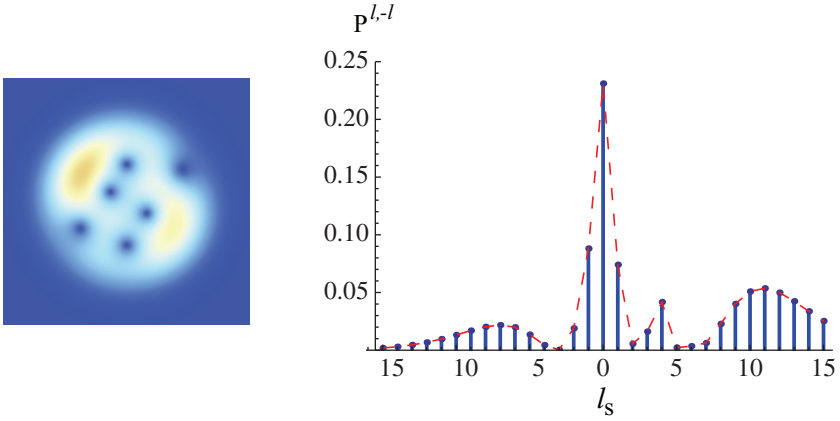

Figure 7. A pump containing six PSs, as described in [18], and the resulting probability amplitudes. The blue lines show the results obtained using equation (14) of [18], while the red line is the result obtained using equations (8) and (12).

be taken into consideration in the calculation as it plays a critical role in the composition of the down-converted state: a state is generally maximally entangled for only one pump-to-signal/idler width ratio.

We first calculate the coincidence amplitudes resulting from a pump that is a superposition of LG modes of equal width, w_p, and complex amplitudes a_n. We can write this as

$$\sum_n a_n \mathrm{LG}_{p_n}^{\ell_n}(\rho,\phi) = a_1 \mathrm{LG}_{p_1}^{\ell_1}(\rho,\phi) + a_2 \mathrm{LG}_{p_2}^{\ell_2}(\rho,\phi) + \cdots, \tag{11}$$

where n labels the modes in the superposition and $\sum_n |a_n|^2 = 1$. The overlap integral (5) then becomes

$$\begin{aligned} C_{p_\mathrm{s},p_\mathrm{i}}^{\ell_\mathrm{s},\ell_\mathrm{i}} &= \sum_n \int_0^{2\pi} \mathrm{d}\phi \int_0^{\infty} \rho\, \mathrm{d}\rho a_n \mathrm{LG}_{p_n}^{\ell_n}(\rho,\phi) \left[\mathrm{LG}_{p_\mathrm{s}}^{l_\mathrm{s}}(\rho,\phi)\right]^* \left[\mathrm{LG}_{p_\mathrm{i}}^{l_\mathrm{i}}(\rho,\phi)\right]^* \\ &= \sum_n a_n C_{n,p_\mathrm{s},p_\mathrm{i}}^{\ell_\mathrm{s},\ell_\mathrm{i}}, \end{aligned} \tag{12}$$

where $C_{n,p_\mathrm{s},p_\mathrm{i}}^{\ell_\mathrm{s},\ell_\mathrm{i}}$ are the coincidence amplitudes, calculated from (8), for each Laguerre–Gaussian component, $|\ell_\mathrm{p}, p_\mathrm{p}\rangle$, of the pump field.

In order to investigate a pump containing PSs we make use of its projection onto LG modes [27]. A field containing N PSs can be written as a superposition of LG modes, $\sum_{\ell=0}^{N} a_\ell \mathrm{LG}_0^\ell$, with complex amplitudes

$$a_\ell = \sqrt{\pi}(-1)^{N-\ell} \left(\frac{w_\mathrm{p}}{\sqrt{2}}\right)^{\ell+1} \sqrt{\ell!}\; b_{N-\ell}, \tag{13}$$

where b_m are given by equation (11) of [18] or, equivalently, by

$$b_m = \frac{1}{m!}\frac{\partial^m}{\partial x^m} \prod_{i=1}^{N} (1 + \rho_i \mathrm{e}^{\mathrm{i}\phi_i} x)|_{x=0} \tag{14}$$

with $m = [0, N]$ and ρ_i and ϕ_i being the radial and azimuthal positions of the PSs, respectively.

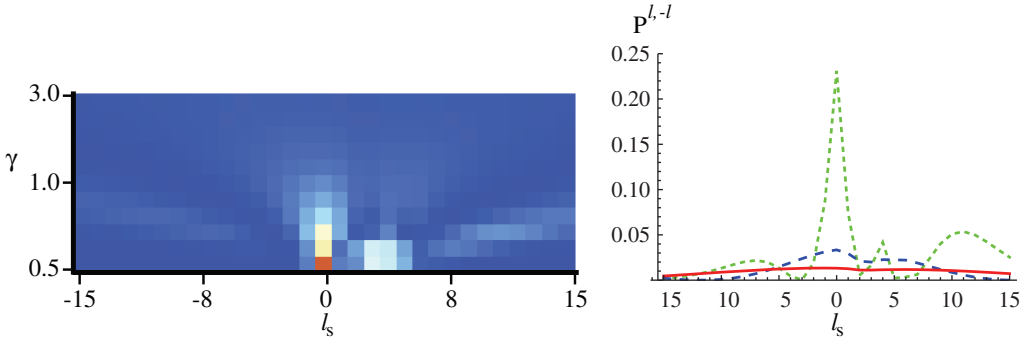

Figure 8. SB for superposition pump for $\gamma_s = \gamma_i = 0.5$ to 3.0 (left) with slices at $\gamma_s = \gamma_i = 1.0$ (green, small dash), 2.0 (blue, large dash) and 3.0 (red, solid) shown on the right.

Following [18], we consider a pump containing six PSs at positions $\rho_1 = 0.65w_p$, $\rho_2 = 1.85w_p$, $\rho_3 = 1.06w_p$, $\rho_4 = 0.54w_p$, $\rho_5 = 1.53w_p$, $\rho_6 = 1.24w_p$ and $\phi_i = i\pi/3$ for $i = 1, 6$. Substituting these values into (13) and then into (12) allows us to calculate the form of the pump, as shown on the left in figure 7, and the resultant coincidence probabilities, vertical (blue) lines shown on the right in figure 7. We find excellent agreement with the results from equation (14) of [18] (dashed red line). We calculated the coincidence probabilities $P^{0,0}_{0,0}$, $P^{1,1}_{0,0}$, $P^{2,2}_{0,0}$, $P^{3,3}_{0,0}$ and confirmed that these were equal and so this pump produces the maximally entangled qu-quart in the subspace $S_4 = \{|0, 0\rangle, |1, 1\rangle, |2, 2\rangle, |3, 3\rangle\}$. Note, however, that in this example we assumed that the pump, signal and idler all had the same width, i.e. $\gamma_s = \gamma_i = 1$. Since we have seen that the composition of the down-converted state is strongly dependent on the ratio of the pump width to the signal and idler widths, we extended these results by calculating the SB as a function of γ, keeping $\gamma_s = \gamma_i$ for simplicity. As expected, we see a large variation in SB for different γ, as shown on the left in figure 8. This can been seen more clearly on the right of figure 8, where we plot the SB at $\gamma = 1.0, 2.0, 3.0$. It is clear that by choosing the mode widths appropriately it is possible to tailor the SB in very different ways.

Changing the relative beam sizes has a large effect on the composition of the entangled state with important implications to the 'engineering' of the down-converted state: states that are maximally entangled for one value of γ are generally not maximally entangled for any other values of γ. To illustrate this we consider the maximally entangled qu-quart produced by the six-PS pump above and calculate the coincidence probabilities $P^{0,0}_{0,0}$, $P^{1,1}_{0,0}$, $P^{2,2}_{0,0}$, $P^{3,3}_{0,0}$ as a function of γ. From figure 9 it is clear that this state is only maximally entangled if $\gamma = 0.5$ or $\gamma = 1.0$. In order to obtain this state, one has to ensure that these conditions are met.

4. Conclusion

We have calculated the exact analytical form of the biphotons produced by SPDC in a thin crystal and under collinear phase matching conditions. Our result has no restrictions on the angular or radial momenta or, in particular, on the width of the pump, signal and idler modes and can be used with any pump that is an LG mode, or a superposition thereof. We have shown that OAM is conserved and we find excellent agreement with previous analyses that considered more restricted conditions.

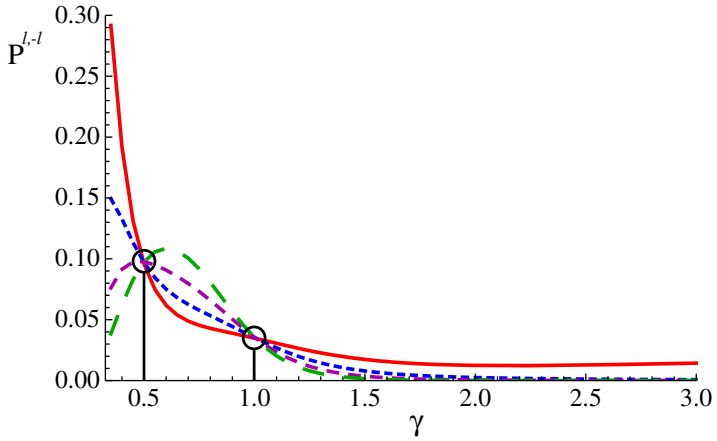

Figure 9. Normalized coincidence probabilities $P_{0,0}^{0,0}$ (red, solid), $P_{0,0}^{1,1}$ (blue, small dash), $P_{0,0}^{2,2}$ (magenta, medium dash) and $P_{0,0}^{3,3}$ (green, large dash) as a function of γ. These are equal and so the state is maximally entangled for only two values of γ, $\gamma = 0.5$ and 1.0, as indicated by the circles.

We used our result to calculate the SB for a variety of pumps and demonstrated the influence of various beam parameters, in particular the pump width and the choice of LG base for the signal and the idler, on the resulting coincidence amplitudes.

In particular, we demonstrated the importance of beam widths when calculating engineered entangled states and showed that maximal entanglement is dependent both on the form of the pump and on the ratio of the beam widths. We suggest that this is an important consideration and may also offer another degree of freedom in quantum communications.

Spontaneous parametric down-conversion is a very wide area of research and so we have necessarily limited ourselves to the thin crystal, collinear phase matching conditions, which are the regimes of importance to many current experiments in this area. Indeed, we have shown previously that our results can be applied to the non-collinear setup for crystal lengths up to tens of centimetres. Extension to non-collinear systems and thick crystals, where phase matching and the effects such as spatial walk-off should be included, is a suitable topic for future analysis.

Acknowledgments

This research was supported by the DARPA InPho program through the US Army Research Office award W911NF-10-1-0395 and by the UK Engineering and Physical Sciences Research Council (EPSRC). I particularly thank Stephen Barnett, Gian-Luca Oppo and Shashank Virmani for useful discussions.

References

[1] Plenio M B and Virmani S 2007 *Quantum Inf. Comput.* **7** 1
[2] Barnett S M 2009 *Quantum Information* (New York: Oxford University Press)
[3] Neilsen M and Chuang I L 2000 *Quantum Computation and Quantum Information* (Cambridge: Cambridge University Press)
[4] Ursin R *et al* 2007 *Nat. Phys.* **3** 481

[5] D'Angelo M, Kim Y H, Kulik S P and Shih Y 2004 *Phys. Rev. Lett.* **92** 233601
[6] Bennink R S, Bentley S J, Boyd R W and Howell J C 2004 *Phys. Rev. Lett.* **92** 033601
[7] Pittman T B, Shih Y H, Strekalov D V and Sergienko A V 1995 *Phys. Rev.* A **52** R3429
[8] Kolobov M I (ed) 2007 *Quantum Imaging* (Singapore: Springer)
[9] Mair A, Vaziri A, Weihs G and Zeilinger A 2001 *Nature* **412** 313
[10] Jack B, Yao A M, Leach J, Romero J, Franke-Arnold S, Ireland D G, Barnett S M and Padgett M J 2010 *Phys. Rev.* A **81** 043844
[11] Leach J, Jack B, Romero J, Jha A K, Yao A M, Franke-Arnold S, Ireland D G, Boyd R W, Barnett S M and Padgett M J 2010 *Science* **329** 662
[12] Hong C K and Mandel L 1985 *Phys. Rev.* A **31** 2409
[13] Arlt J, Dholakia K, Allen L and Padgett M J 1998 *J. Mod. Opt.* **45** 1231
[14] Leach J, Dennis M R, Courtial J and Padgett M J 2005 *New J. Phys.* **7** 55
[15] Romero J, Leach J, Jack B, Dennis M R, Franke-Arnold S, Barnett S M and Padgett M J 2011 *Phys. Rev. Lett.* **106** 100407
[16] Torres J P, Alexandrescu A and Torner L 2003 *Phys. Rev.* A **68** 050301
[17] Ren X F, Guo G P, Yu B, Li J and Guo G C 2004 *J. Opt. B: Quantum Semiclass. Opt.* **6** 243
[18] Torres J P, Deyanova Y and Torner L 2003 *Phys. Rev.* A **67** 052313
[19] Saleh B E A, Abouraddy A F, Sergienko A V and Teich M C 2000 *Phys. Rev.* A **62** 043816
[20] Barnett S M and Zambrini R 2007 *Quantum Imaging* ed K I Kolobov (Singapore: Springer) p 284
[21] Franke-Arnold S, Barnett S M, Padgett M J and Allen L 2002 *Phys. Rev.* A **65** 033823
[22] Gradshteyn I S and Ryzhik I M 1980 *Table of Integrals, Series and Products* (London: Academic) see equation 8.970 (1) p 1037
[23] Miatto F M, Yao A M and Barnett S M 2010 *Phys. Rev.* A **83** 033816
[24] Kaszlikowski D, Gnacinski P, Zukowski M, Miklaszewski W and Zeilinger A 2000 *Phys. Rev. Lett.* **85** 4418
[25] Collins D, Gisin N, Linden N, Massar S and Popescu S 2002 *Phys. Rev. Lett.* **88** 040404
[26] Brambilla M, Battipede F, Lugiato L A, Penna V, Prati F, Tamm C and Weiss C O 1991 *Phys. Rev.* A **43** 5090
[27] Indebetouw G 1993 *J. Mod. Opt.* **40** 73